PERGAMON

Journal of Structural Geology 25 (2003) 765–779

JOURNAL OF STRUCTURAL GEOLOGY

www.elsevier.com/locate/jstrugeo

Structural style and tectonic significance of the Jianglang dome in the eastern margin of the Tibetan Plateau, China

Dan-Ping Yan[a,b], Mei-Fu Zhou[b,*], Honglin Song[a], Zhaoren Fu[a]

[a]*Faculty of Geology and Mineral Resources, China University of Geosciences, Beijing, China*
[b]*Department of Earth Sciences, University of Hong Kong, Hong Kong SAR, China*

Received 22 February 2001; accepted 29 April 2002

Abstract

The Jianglang Tectonic Dome (JTD) lies on the eastern margin of the Tibetan Plateau and consists of three tectono-stratigraphic units separated by two extensional detachment faults: a schist complex, a middle ductile slab and an overlying sedimentary unit. The schist complex is composed of quartz–mica schists and amphibolites of possible Mesoproterozoic age and exhibits two early foliations (S_1 and S_2) overprinted by two later foliations (S_3 and S_4). The ductilely deformed middle slab consists of Paleozoic quartzite, phyllite, marble, amphibolite and meta-basalt. It is characterized by pervasive intrafolial and intraformational recumbent folds with a penetrative axial foliation S'_1 (an equivalent of S_3 in the basement rocks). The cover unit, the Triassic Xikang Group of flysch sedimentary rocks, experienced shallow level buckling and flattening deformation with an axial cleavage defining S''_1 (an equivalent of S_4 in the middle slab and basement rocks).

The JTD appears to have experienced three stages of extension immediately after orogeny. The earliest (D_1), recorded by an axial surface S_1 of S_0 intrafolial folds and sub-parallel to S_0 in the schist complex, probably occurred prior to the collision between the South China and North China Blocks. This extensional event was followed by subduction of the Yangtze Block to the west towards the eastern margin of the Tibetan Plateau. The two detachment faults are characterized by structures formed by ductile–brittle to brittle shear deformation, which are sub-parallel to the layer of S_2 in the lower detachment and to S_0 in the upper detachment. These faults mark the second stage of extension and may have caused thinning and selective removal of the Sinian and Paleozoic strata, as well as exhumation of the schist complex and the middle slab in the middle Jurassic (177 Ma). The final stage of extension (D_5), shown by brittle deformation and thermo-metamorphism from the lower detachment to the Xikang Group, was associated with the Indian–Eurasia collision.
© 2002 Elsevier Science Ltd All rights reserved.

Keywords: Jianglang Tectonic Dome; Schist complex; Ductile slab; Sedimentary unit; Tibet; South China

1. Introduction

Recent studies in the eastern margin of the Tibetan Plateau have identified a group of distinctive, isolated, domal metamorphic bodies, including the Motianling, Qiaoziding, Xunlongbao; Yaside, Gongcai, Gezong, Taka, Jianglang, Changqiang, Qiasi and Penguan metamorphic complexes (Fig. 1) (Hou, 1996; Huang et al., 1996; Song et al., 1996; Yan et al., 1996, 1997; Fu et al., 1997). Chinese geologists classified these bodies as gneissic and structural domes and magmatic core complexes (Hou et al., 1996; Huang et al., 1996). The diversity of interpretation probably reflects variable exposures of structural components of extensional tectonic domes. Previous studies noted that there are significant stratigraphic omissions of Sinian through Ordovician units around these domal metamorphic terranes (Fig. 2) (SBGMR, 1991). The metamorphic terranes were previously thought to represent a paleo-uplift that resulted in the variable omissions (SBGMR, 1991). Xu et al. (1992) considered these metamorphic blocks to be tectonic slices, possibly related to the collision of India to Eurasia. However, the characteristics of these domal complexes and their relationship to the regional geology were not clear.

The JTD is well known in China because it contains hydrothermal Cu-sulfide deposits (Fu et al., 1997). We carried out an extensive field mapping program in the Jianglang area. On the basis of detailed field observations, this paper presents new tectono-stratigraphic data that reveal the structural style of the JTD. We further discuss

* Corresponding author. Tel.: +852-2857-8251; fax: +852-2517-6912.
E-mail address: mfzhou@hkucc.hku.hk (M.F. Zhou).

0191-8141/03/$ - see front matter © 2002 Elsevier Science Ltd All rights reserved.
PII: S0191-8141(02)00059-7

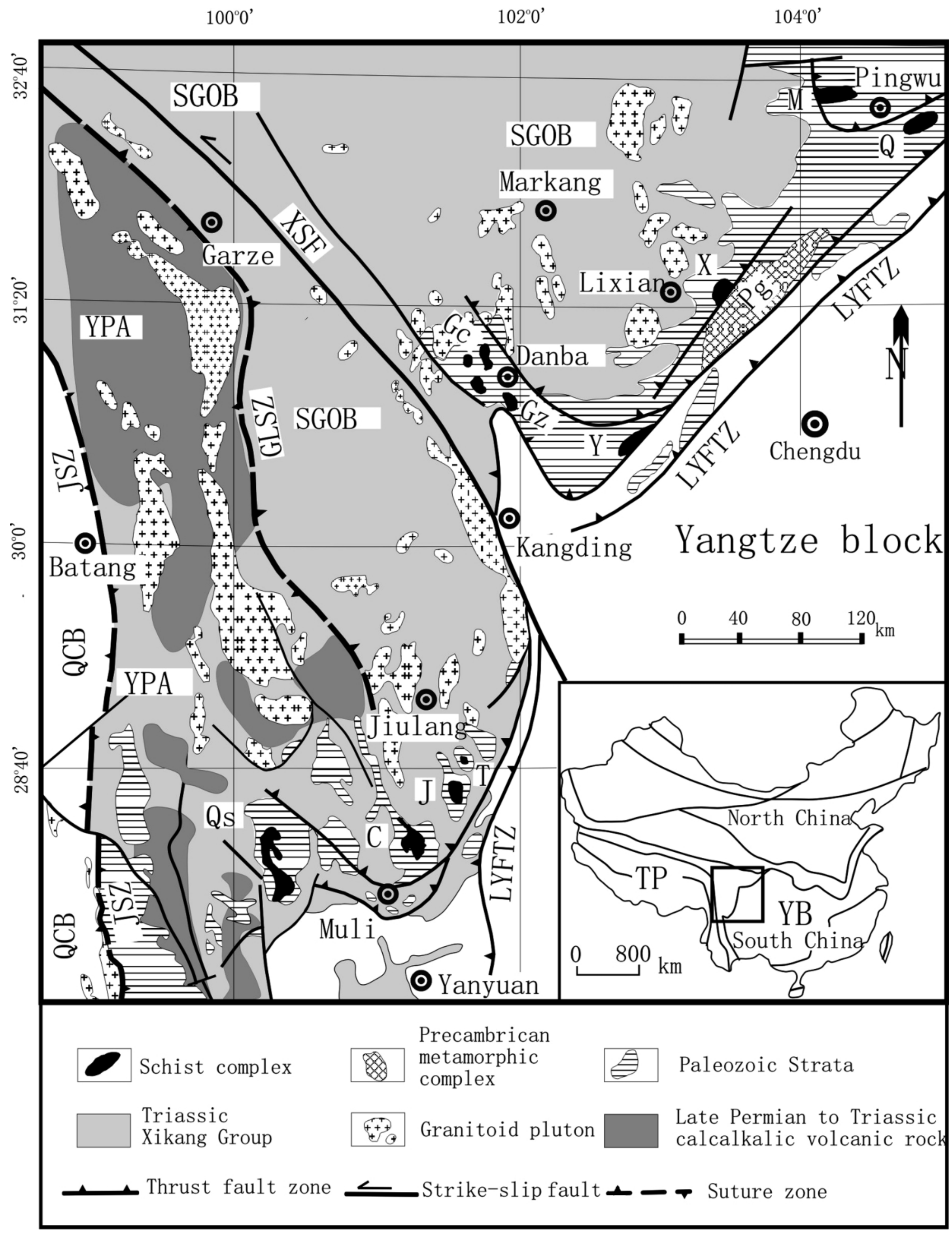

Fig. 1. Geological map of the eastern margin of the Tibetan Plateau, showing the Longmenshan–Yanyuan Foreland Thrust Zone (LYFTZ) and the distribution of tectonic domes. Tectonic units: the Songpan–Garze Orogenic Belt (SGOB); the Yidun Paleozoic Arc (YPA); and the Qiangtang–Changdu Block (QCB). Major sutures and faults: the Jingshajiang Suture Zone (JSZ); the Garze–Litang Suture Zone (GLSZ); the Xianshuihe sinistral Strike-slip Fault (XSF). Major metamorphic complexes (domes): Motianlin (M); Qiaoziding (Q); Xunlongbao (X); Yaside (Y); Gezong (Gz); Gongcai (Gc); Taka (T); Jianglang (J); Changqiang (C); Qiasi (Qs); and Pen-guan (base map from SBGMR (1991) and Luo et al. (unpublished)).

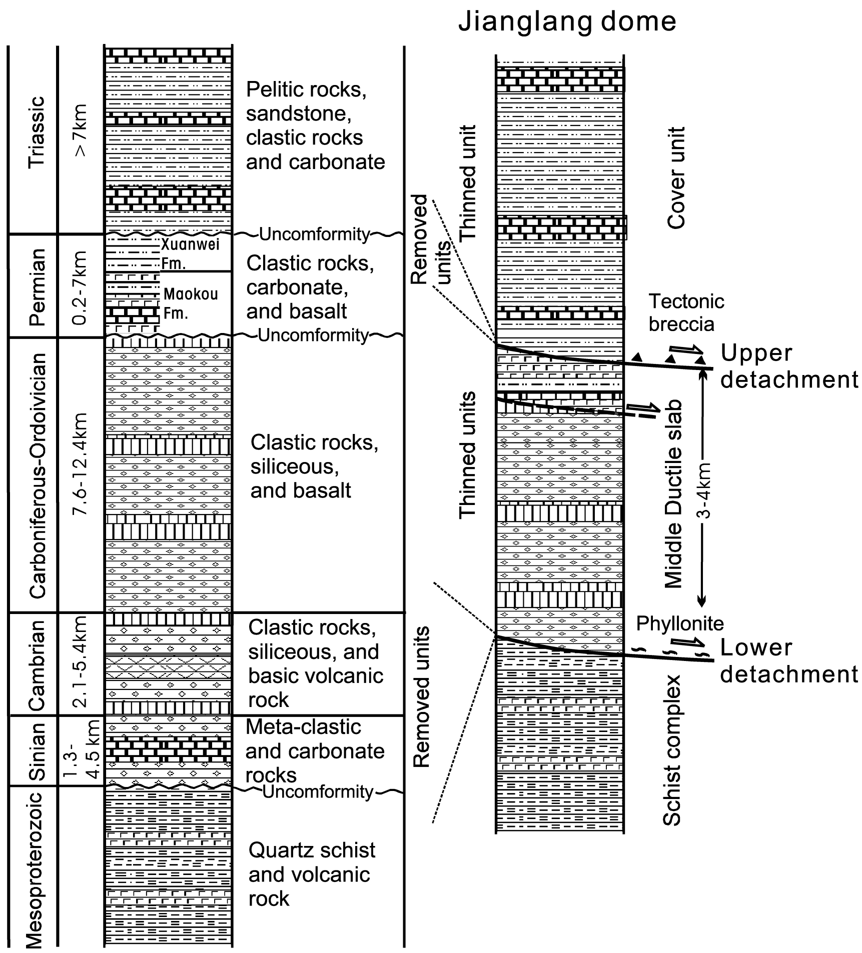

Fig. 2. Generalized stratigraphic column of the Songpan–Garze orogenic belt and tectono-stratigraphic correlations in the Jianglang tectonic dome (data for the regional stratigraphic column are from SBGMR (1991)).

its deformation sequence and tectonic significance in the understanding of the regional geology of the eastern margin of the Tibetan Plateau.

2. Geological background

The tectonic framework of the region comprises the Himalayan–Kunlun Tectonic Domain (HKTD) to the west and the Yangtze Block to the east (Fig. 1). Within HKTD, the Songpan–Garze Orogenic Belt (SGOB) is separated from the so-called 'Yidun Paleozoic Arc' by the Garze–Litang suture zone. Further to the west is the Qiangtang–Chongdu Block separated by the Jingshajiang Suture Zone (JSZ) from the 'Yidun Arc' (Fig. 1) (SBGMR, 1991; Mattauer et al., 1992; Xu et al., 1992; Yan et al., 1997; Chang, 2000; E. Wang and Burchfiel, 2000; X. Wang et al., 2000).

The SGOB is made up of a thick sequence (ca. 7 km) of flysch-type sedimentary rocks which form the Triassic Xikang Group (Nie et al., 1994, 1995; Avigad, 1995; Bruguier et al., 1997; Chang, 2000) and a thick Sinian and Paleozoic sequence (>10 km) of flysch clastic rocks and mafic volcanic rocks (Fig. 2). The Longmenshan and Yanyuan Foreland Thrust Zone (LYFTZ), as part of the SGOB, forms the easternmost part of the Tibetan Plateau and separates it from the Yangtze Block (Liu et al., 1994; Burchfiel et al., 1995; Chen et al., 1995; Chen and Wilson, 1996; Lacassin et al., 1996; Worley and Wilson, 1996 (Fig. 1). On a regional scale, the Xianshuihe sinistral strike-slip fault (XSF) has produced sinistral displacement of about 60 km between the Longmenshan and Yanyuan Foreland Thrust Zones during the collision between India and Eurasia (Allen et al., 1991; Roger et al., 1995; E. Wang et al., 1998) (Fig. 1). Several tectonic domes lie in the hinterland of the Longmenshan and Yanyuan thrust zone within the SGOB (Song et al., 1996; Yan et al., 1997).

To the east, the Yangtze Block consists of a Paleoproterozoic to Mesoproterozoic basement overlain by a Neoproterozoic (Sinian) to Cenozoic cover. Paleoproterozoic strata are known as the Huili Group or its equivalents. These consist of supracrustal rocks metamorphosed to greenschist facies and locally to

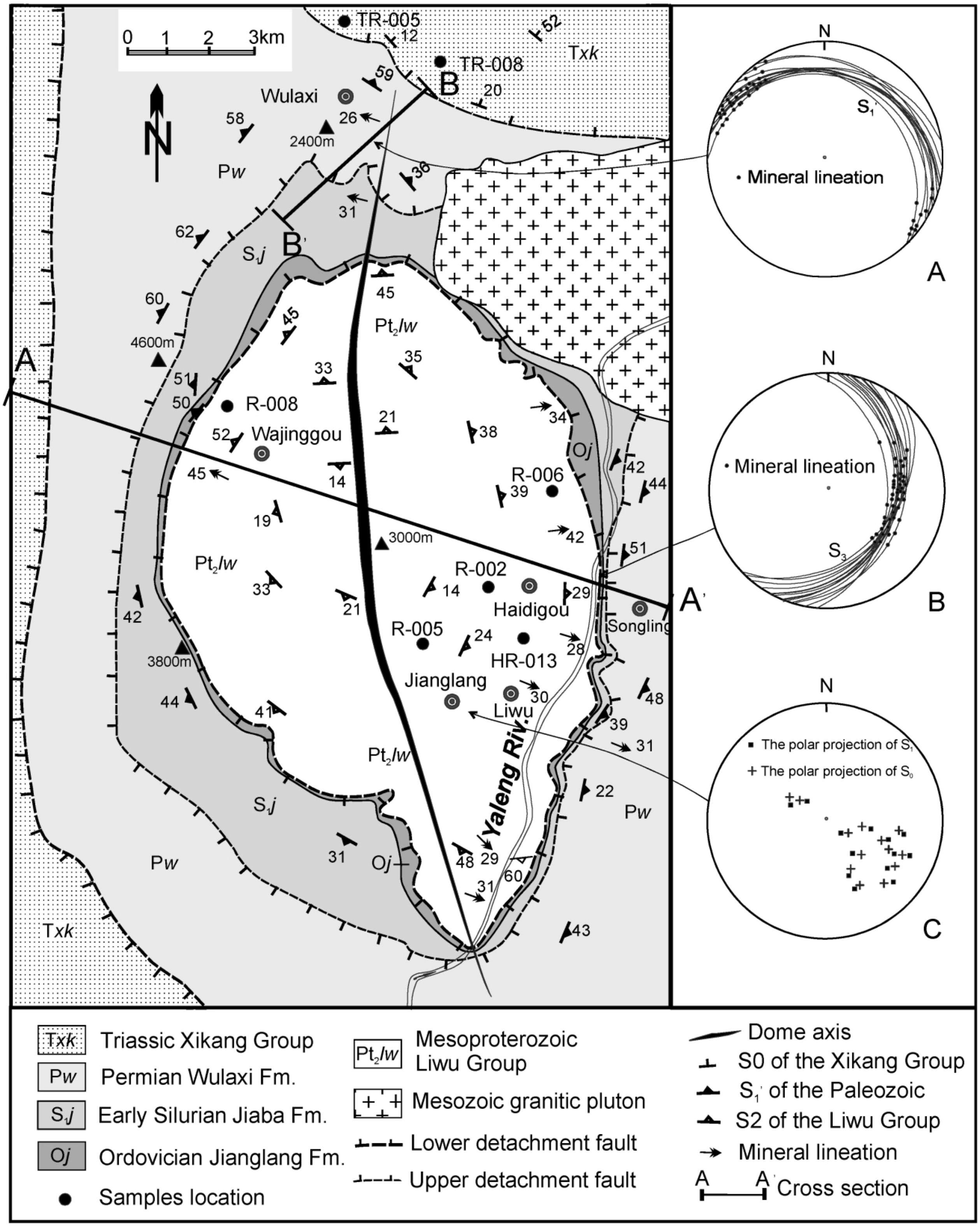

Fig. 3. A structural map of the Jianglang dome. Insets A and B show the mineral lineation on S'_1 of the Wulaxi Formation in the middle ductile slab and on S_3 of the detachment fault. Inset C is a lower hemisphere Wolff net showing the polar projections of S_0 and S_1 from Liwu. The two sets are almost superposed. The dashed arcs represent foliation S'_1 (inset A) and S_3 (inset B). The smaller black dots in the Wulff net are the mineral lineations. The heavy black dots on the map show the locations of samples collected for metamorphic analysis and isotopic age determination.

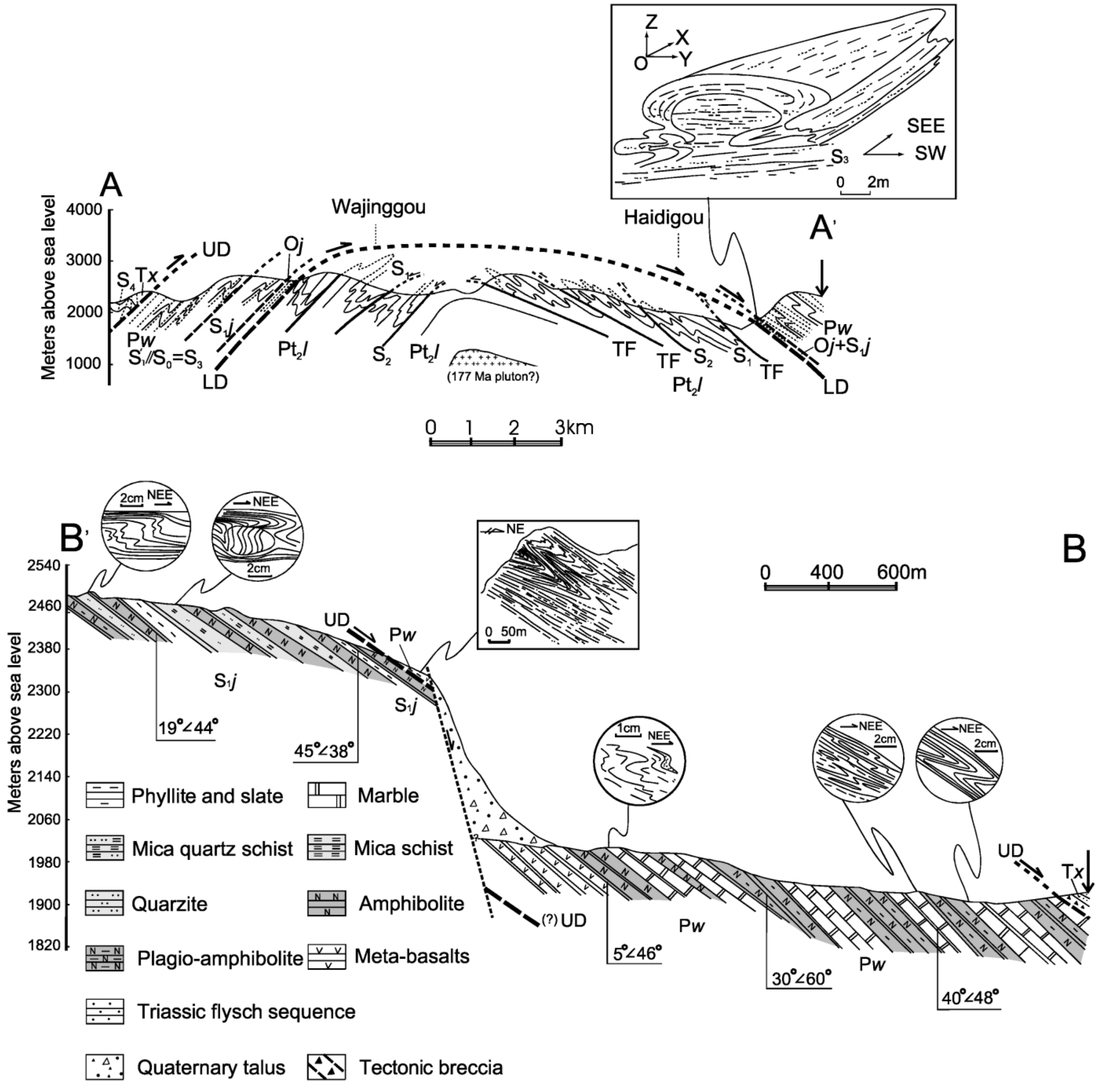

Fig. 4. Cross-sections through the JTD (locations shown in Fig. 2). Section A–A′ shows the structural style of the schist complex and its relationship with the cover sequence. Note the three-dimensional sketch of an 'A' type fold (sheath fold) with *XYZ* coordinate showing the observed section and the shear sense in the lower detachment fault. Section B–B′ (note that the scale is different from that in Fig. 2) shows the structural style and the ESE sense of movement of the ductile deformation in the middle ductile slab and the brittle deformation in the upper detachment fault. The sketch with section B–B′ shows intra-folds, also called 'folding layer' by Song et al. (1996), and give the shear sense in the middle ductile slab. T*x*: Triassic Xikang group; P*w*: Permian Wulaxi formation; S_1j: early Silurian Jiaba formation; O*j*: Ordovician Jianglang formation; Pt_2l: Mesoproterozoic Liwu group. LD: lower detachment; UD: upper detachment; TF: thrust fault. S_0: sedimentary layer; S'_1, S_1, S_2, S_3 and S_4 are the foliations.

amphibolite and granulite facies. The rocks include paragneiss, mica-schist, graphite-bearing sillimanite–garnet pelitic gneiss (Khondalite), amphibolite, marble, and quartzite. This sequence is overlain by a thick Sinian to Permian sequence (> 10 km) comprising clastic, carbonate, and meta-volcanic rocks (Zhang et al., 1990; SBGMR, 1991; Mattauer et al., 1992; Xu et al., 1992). There are also widespread Late Permian continental flood basalts. These voluminous rocks cover an area of more than 2.5×10^5 km^2 and are interpreted to be the products of a late Permian mantle plume (Chung and Jahn, 1995; Song et al., 2001).

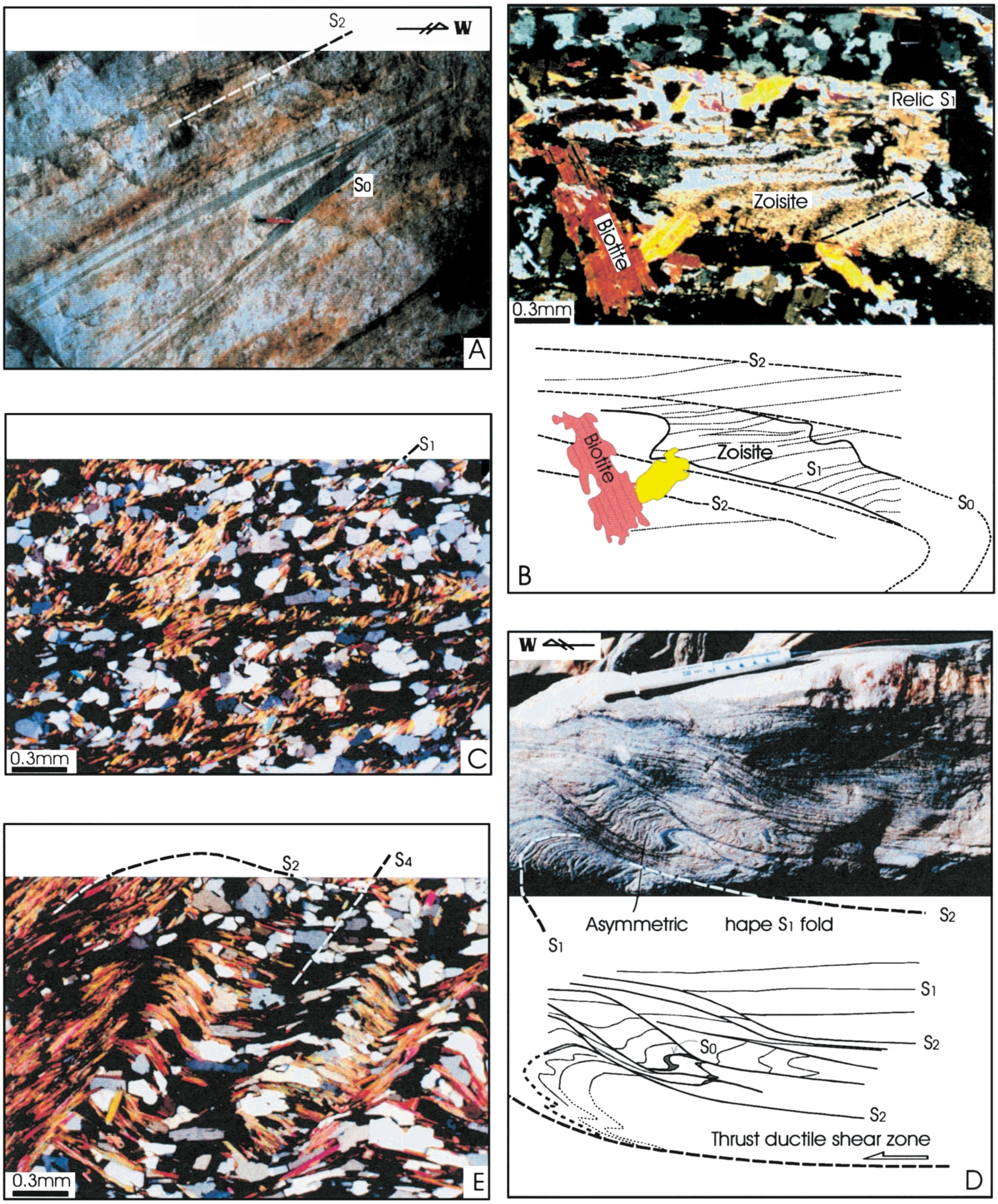

3. Tectono-stratigraphy and structural style of the JTD

The JTD is composed of three units that form a dome-like antiform 18 km long in a north–south direction and 11 km wide (Figs. 3 and 4): a schist complex locally known as the Liwu Group, an overlying ductilely deformed middle slab of Sinian and Paleozoic meta-sedimentary and meta-basaltic rocks, and the Xikang Group, a Triassic cover unit

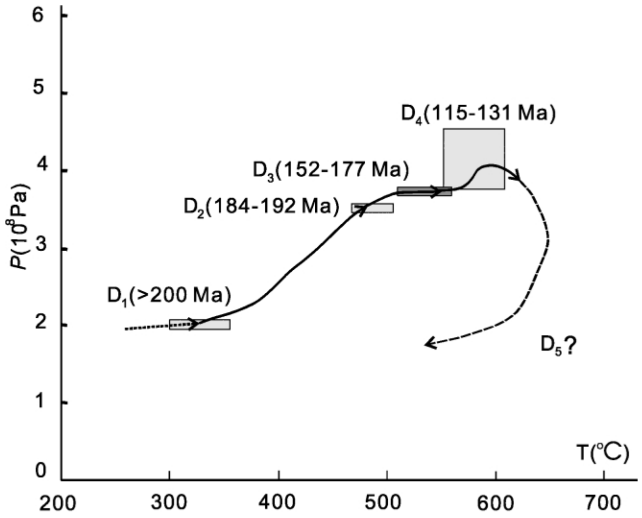

Fig. 6. *P–T–t* path shows the evolution of the JTD. The data of *P*, *T* and *t* are after Song et al. (1996); Yan et al. (1996, 1997) and this study and are discussed in the text. Some of the samples for mineral assemblage and isotopic age determination are shown in Fig. 3.

of weakly metamorphosed sedimentary rocks (Fig. 2). Major detachment faults interpreted as extensional in origin separate the middle slab from both the schist complex and the cover sedimentary rocks. There are also numerous detachment faults within the middle slab.

3.1. Schist complex

The schist complex of the JTD consists of quartz–mica schists and amphibolites of possible Mesoproterozoic age. This sequence is called the Liwu Group, interpreted to be a metamorphic product of the Huili Group within the Yangtze Block. It is characterized by multiphase metamorphism and deformation including foliation transposition. Two early generations of foliations are recognized and these were overprinted by two late generations.

Relict meta-carbonaceous pelitic layers (possibly original bedding S_0) are locally preserved (Fig. 5A). The S_1, a foliation defined by alternating layers of mica-rich and quartz-rich lamellae, is a well-developed schistosity along the axial planes of folded layers between relatively competent layers of S_0. In the coarse-grained schist with an S_0 microfold defined by sericite and zoisite, the foliation S_1 in the hinge zone is a zonal crenulation schistosity (Fig. 5B). The mineral assemblage of S_1 consists mainly of muscovite and quartz with minor biotite, albite, K-feldspar and garnet. Quartz is mainly polygonal and rectangular (Fig. 5C). This mineral assemblage belongs to the upper greenschist facies and is comparable with biotite and garnet zones of the Barrovian sequence and yields temperatures of 300–360 °C and a pressure of 2.0×10^8 Pa (Song et al., 1996; Yan et al., 1997) (Fig. 6).

On a macro scale, S_1 is sub-parallel to the bulk lithological layers of S_0 (Fig. 5D) and is an axial surface schistosity of S_0 intrafolial folds. S_0 and S_1 are sub-parallel to each other (the inset C of Fig. 3), suggesting that the D_1 deformation forming S_1 might be produced by sub-horizontal ductile shear under an extensional regime.

The major foliation, S_2, is an axial surface foliation of recumbent folds of S_1 and is also a shear foliation of reverse ductile shear zones along the overturned limbs of S_1 folds (Fig. 5D). S_2 in hinge zones of S_1 folds shows a symmetric zonal crenulation schistosity and is perpendicular to S_1. Toward the limbs of S_1, folds, S_2, formed along the axial surface of S_1 second-order asymmetric folds ('S'- or 'Z'-shaped), gradually becomes zonal crenulation schistosity, and finally a discrete crenulation schistosity parallel to S_1 (Fig. 5D). A mica-rich and quartz-rich layering (M and Q domains) structure also defines S_2 (Fig. 5C and D).

There are relics of mica-rich lamellae of S_1 in the Q domain of S_2. There are also newly formed biotite grains that are oriented parallel to S_2 in the M domain of S_2 (Fig. 5C and E). The mineral assemblage of S_2 consists mainly of biotite, muscovite and quartz and belongs to the amphibolite facies. Garnet porphyroblasts occur in meta-pelitic rocks. Garnet–biotite and muscovite geothermometers yield temperatures of 460–500 °C and a pressure of 3.5×10^8 Pa (Yan et al., 1997).

A westward sense of movement can be inferred for the shear that produced S_2 from the vergence of recumbent folds and ductile shear zones (Fig. 5D). This tectonic event has K–Ar ages of 192 and 184 Ma using S_2 biotite separates from samples HR-013 and R-005 (Fig. 3), suggesting a correlation with the Indosinian orogeny.

Foliation S_3, clearly developed along the lower detachment zone, is also visible in upper part of the schist complex (see description in Section 3.3).

Foliation S_4 is defined by cleavages across symmetric microfolds of S_2 (Fig. 5E). S_4 is also characterized by newly formed biotite porphyroblasts separating the microlithons. These porphyroblasts are closely packed, with (001) of individual grains roughly perpendicular to S_2. The assemblage of staurolite and biotite or hornblende and plagioclase

Fig. 5. Outcrop-scale and micro-scale structural features of the schist complex of the Liwu Group: (A) Amphibolite relic layers (possibly S_0 bedding) in a mica–quartz schist. The original layers were replaced by S_1 foliation. (B) A limb of a zoisite–sericite schist in a mica–quartz schist, showing the relationship of S_0, S_1, S_2, and later biotite porphyroblasts. (C) The relationship of S_1 to S_2 in the muscovite–quartz schist. The relic of S_1 can be seen by the arrangement of muscovite between the Q-domain of S_2. The rectangular quartz parallel to S_2 reflects an annealing recrystallization after the formation of S_2. (D) Asymmetric folding and westward-directed ductile shear zone shown in a mica–quartz schist and amphibolite. On the limbs of S_1 folds S_2 gradually becomes an asymmetric 'S'-shaped zonal crenulation schistosity, and finally becomes a discrete crenulation schistosity parallel to S_1. Toward the hinge zone of S_1 (westward) folds, S_2 shows a symmetric zonal crenulation schistosity and is perpendicular to S_1. (E) S_4 is represented by crenulation with symmetric microfolds of S_2.

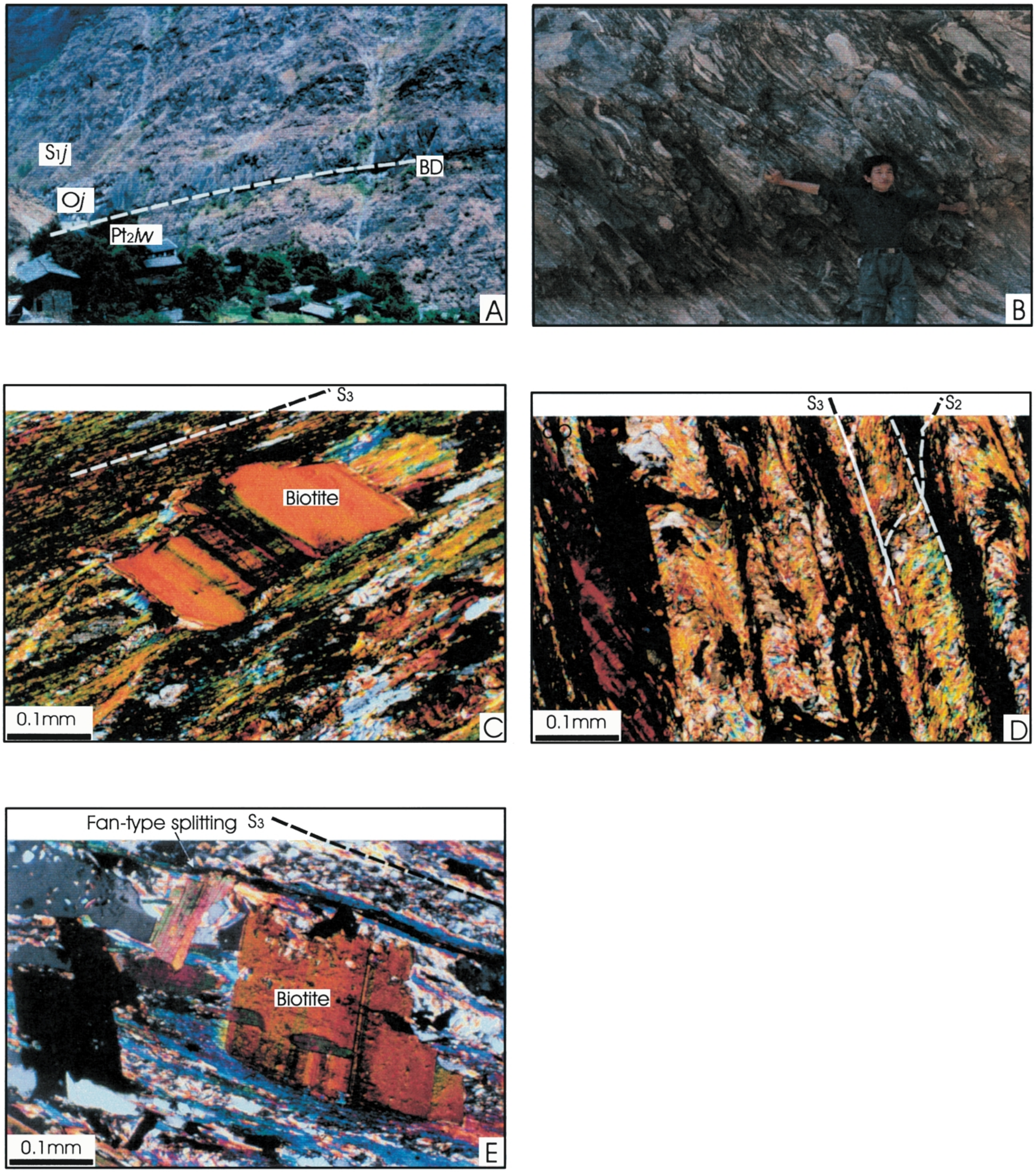

Fig. 7. Ductile deformation of the lower detachment shear zone. (A) A field picture shows the lower detachment shear zone separating the quartzite of the Ordovician Jianglang Formation (O*j*) from the schist complex of the Liwu Group (Pt_2lw). (B) A field picture of the lower detachment shear zone showing elongated clasts in conglomerate after ductile deformation. (C) A biotite porphyroblast with (001) perpendicular to S_3 shows no deformation and is a retrograde product. (D) The relationship among S_2, S_3 and a biotite grain in phyllonite from the lower detachment zone. The parallel arrangement of sericite defines the phyllitic cleavage S_3, whereas the relic of folded S_2 can be seen in the microlithon of S_3. (E) A biotite porphyroblast shows kinking and fan-type splitting along (001) which is perpendicular to S_3.

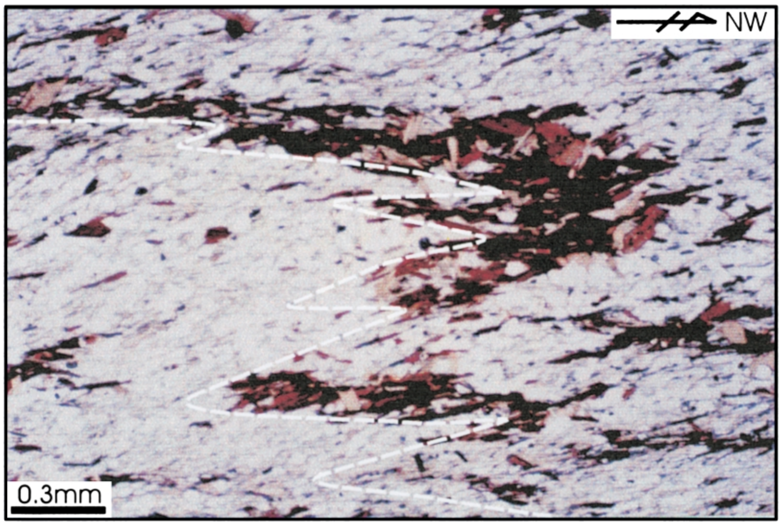

Fig. 8. Micro-intra-formational folding is shown by biotite and quartz in phyllites of the middle ductile slab.

yield temperatures of 550–620 °C and pressures of 4.0–5.0 × 10^8 Pa (Yan et al., 1997) (Fig. 6).

Disoriented staurolite porphyroblasts that occur along the foliation surface of S_2, as well as later biotite porphyroblasts in the cover rock, represent a later low-grade greenschist facies metamorphism.

The schist complex experienced multiphase deformation under both extensional and compressional regimes. The first deformation (D_1) produced sub-horizontal shears, probably under the extensional regime, forming the folding layer structures and S_1 foliation. The second deformation (D_2) produced the westward vergent S_1 folds and reverse ductile shear (S_2) zones by E–W compression.

3.2. Lower detachment zone

The lower detachment zone is composed of phyllonite to mylonite and separates the schist complex from the middle slab (Figs. 3, 4 and 7A). This zone varies in thickness from only 10 cm in the east (Fig. 7A) to about 40 cm in the west, and marks a transitional change from the schist complex to the middle slab. Foliation S_3 of the detachment has a phyllonitization structure in outcrop, such as elongated clasts in conglomerate (Fig. 7B) and deformation of biotite along the (001) crystal face (Fig. 7C). Under the microscope there are a series of discrete crenulation cleavages (Fig. 7D). Within microlithons of S_3, the differential layer S_2 can be distinguished by the transverse arrangement of quartz-rich and sericite-rich layers (Fig. 7D). The latter is thought to be the altered product of muscovite. New grains of muscovite and biotite parallel to S_3 imply a greenschist facies metamorphism (Fig. 7E). Two kinds of biotite porphyroblasts with their (001) planes perpendicular to S_3 are commonly present (Fig. 7C and E). One set, which was later deformed by shear to produce kinking, pressure shadows (Fig. 7C) and fan-type splitting of biotite (Fig. 7E), is believed to represent a stage of brittle–ductile deformation. The other set is not deformed (Fig. 7C). These characteristics reflect multiphase deformation along the lower detachment fault.

Sheath folds, exposed on the eastern part of this zone (inset on top right corner of section A–A′ in Fig. 4) and mainly marked by quartz–muscovite schist, show the sense and direction of shear. On a *YOZ* section, the phyllonite foliation S_3 is the axial-plane foliation of S_2 folding, and the folds are 'Ω' type or circle type. On a *XOZ* section the fold are asymmetric 'Z' type with the hinge tip to the shear direction. Measurement of mineral lineations on S_3, which are parallel to the axes of 'Ω' type folds, indicates that *X*-axes point to the E–SE (98–110°) (Fig. 3B), also representing the shear direction.

This zone is overlain directly by Ordovician quartzites (Fig. 4) with omission of Sinian and Cambrian strata which outcrop on the periphery of the Jianglang area (Fig. 2). Therefore, we interpret it as a low-angle normal detachment fault formed by extension tectonicsYin, 1989 (Spencer, 1984; Yin, 1989; Wernicke et al., 1988; Lister et al., 1991).

3.3. Middle ductilely deformed slab

The middle, ductilely deformed slab, which is separated from the schist by the lower detachment fault (Figs. 3 and 4), consists of three Paleozoic formations that crop out around the schist complex. The lowermost Jianglang Formation of quartzite is correlated with similar strata in the Changqiang and Qiasi tectonic domes (Figs. 1 and 2), which are assigned an Ordovician age (SBGMR, 1991). The middle unit is the Jiaba Formation of phyllite assigned an early Silurian age based on regional stratigraphic correlation (SBGMR, 1991). The uppermost Permian Wulaxi Formation consists of meta-basalts with an interbedded assemblage of amphibolite and marble.

The middle slab shows greenschist to amphibolite facies metamorphism under temperatures of 510–555 °C and a

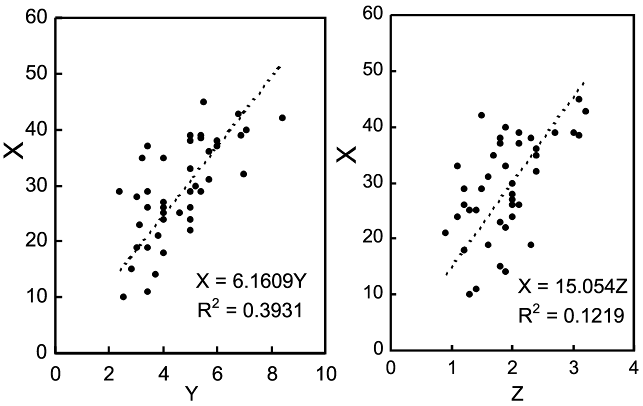

Fig. 9. *Y* versus *X* and *Z* versus *X* of finite-strain of the pebble marble from the Permian Wulaxi Formation. Dashed lines are the best fit lines.

pressure of 3.8×10^8 Pa, calculated using hornblende–plagioclase geothermometry (Yan et al., 1997) (Fig. 6). It represents a metamorphosed supra-crustal sequence. Original sedimentary structures in meta-sedimentary rocks are preserved locally. The structural style is characterized by: (1) pervasive development of intra-folial or intra-formational recumbent folds in the original bedding layers (insets of Figs. 4 and 8) with amplitudes and wavelengths ranging from microscopic to outcrop scale; (2) pervasive development of penetrative foliation S'_1, which represents axial planar cleavages of recumbent folds, sub-parallel to the original bedding; (3) ductile shear zones in incompetent layers, which formed phyllonites and blasto-mylonites; and (4) numerous detachment faults with southeast–eastward normal sense of movement within the sequence (Fig. 3), which thinned or removed some of the Sinian and Paleozoic units. A strong ductile deformation is demonstrated by finite-strain measurements from deformed pebbles in these shear zones that show ratios of *X*/*Z* up to 15:1 and *X*/*Y* up to 6:1 (Fig. 9).

Mineral lineations on S'_1 foliation cluster statistically between 290 and 300° in Wulaxi (Fig. 3). When the S'_1 foliation is restored to horizontal (presuming the strata was horizontal before deformation), the direction is the same as the mineral lineation on the phyllonite foliation S_3 of the lower detachment and the top part of the schist complex (Fig. 3A and B).

3.4. Upper detachment zone

The upper detachment zone, mainly composed of breccia with chlorite on the surface of frictional sliding, separates the middle slab and the Xikang Group. This zone thinned or removed some of the lower Triassic sequence and the upper Permian Xunwei Formation and placed the brittle deformation directly on the ductilely deformed unit (Fig. 2). The shear direction shown by scratch and calcite raft is southeast–eastward normal sense of movement (Fig. 4).

3.5. Cover sedimentary rocks of the Xikang Group

The cover sedimentary rocks belong to the Triassic Xikang Group, a major component of the SGOB (Fig. 1). The Xikang Group experienced lower greenschist facies metamorphism and is composed of terrigenous flysch with shallow level buckling and flattening deformation (Fig. 10A). The characteristics of the structural style are as follows: (1) the deformational surface is the original bedding surface; (2) the folds in the interbeds of pelite and psammite are subharmonic in profile with type 1B folds in competent sandstone beds and type 1C or type 2 folds in incompetent shale or siltstone beds (Fig. 10A) (cf. Ramsay and Huber, 1987); (3) there is a fan-shaped cleavage S''_1 in the sandstones, whereas inverse fan-shaped or axial plane slaty cleavages occur in the slates. S''_1, however, is not parallel to the original bedding in a regional scale, different from S'_1; (4) axial planes of folds strike N–S and dip steeply, reflecting a regional compression in an E–W direction; and (5) the rocks are locally overprinted by later thermo-metamorphism as shown by biotite porphyoblasts that crosscut the cleavage (Fig. 10B). These are similar to the biotite porphyoblasts in the lower detachment (Fig. 9C). Two biotite separates (samples Tr-005 and Tr-008, sample location in Fig. 3) yield K–Ar ages of 121 and 131 Ma, respectively.

4. Discussion

4.1. Extensional elements in the JTD

In Jianglang, the structural characteristics of the middle slab are typical of brittle to ductile deformation. We suggest that this ductilely deformed middle slab is a special tectono-stratigraphic layer separating the upper cover sedimentary sequence and the schist complex. A three-layered configuration (Fig. 11A and C) can be established for the JTD. These three tectono-stratigraphic layers are similar to the configuration for metamorphic core complexes (MCC) with the middle slab being the fluid crustal layer proposed by Wernicke and Axen (1988) and Wernicke (1990). This configuration is consistent with the rheological stratification of the lithosphere by Rutter (1993) (Fig. 11E).

Although the middle slab and the schist complex show similar metamorphic grades, there are variable omissions of Sinian and Paleozoic strata (Fig. 2). The removal of these strata can be readily explained by the extensional, lower detachment fault. On the other hand, the middle slab shows strong contrast in the metamorphic grade from the sedimentary cover sequence of the Triassic Xikang Group. The Wulaxi Formation in the middle slab is a metamorphic product of the Emeishan Flood basalts and the Middle Permian Maokou carbonate Formation (SBGMR, 1991; Song et al., 2001). On a regional scale, this sequence is overlain by sandstone of the Late Permian Xuanwei

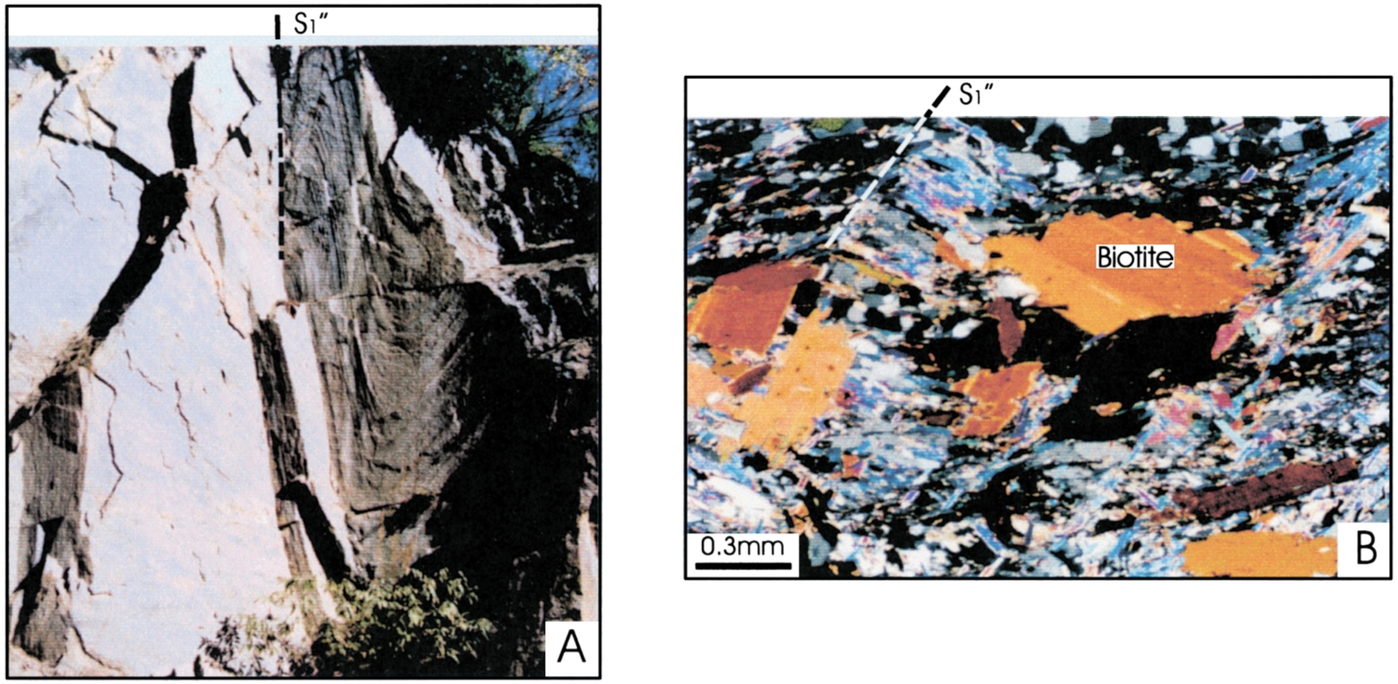

Fig. 10. Structural styles of the Xikang Group. (A) Type 1C folds of incompetent shale and siltstone beds. (B) Biotite porphyoblasts crosscut the cleavage (S'_1).

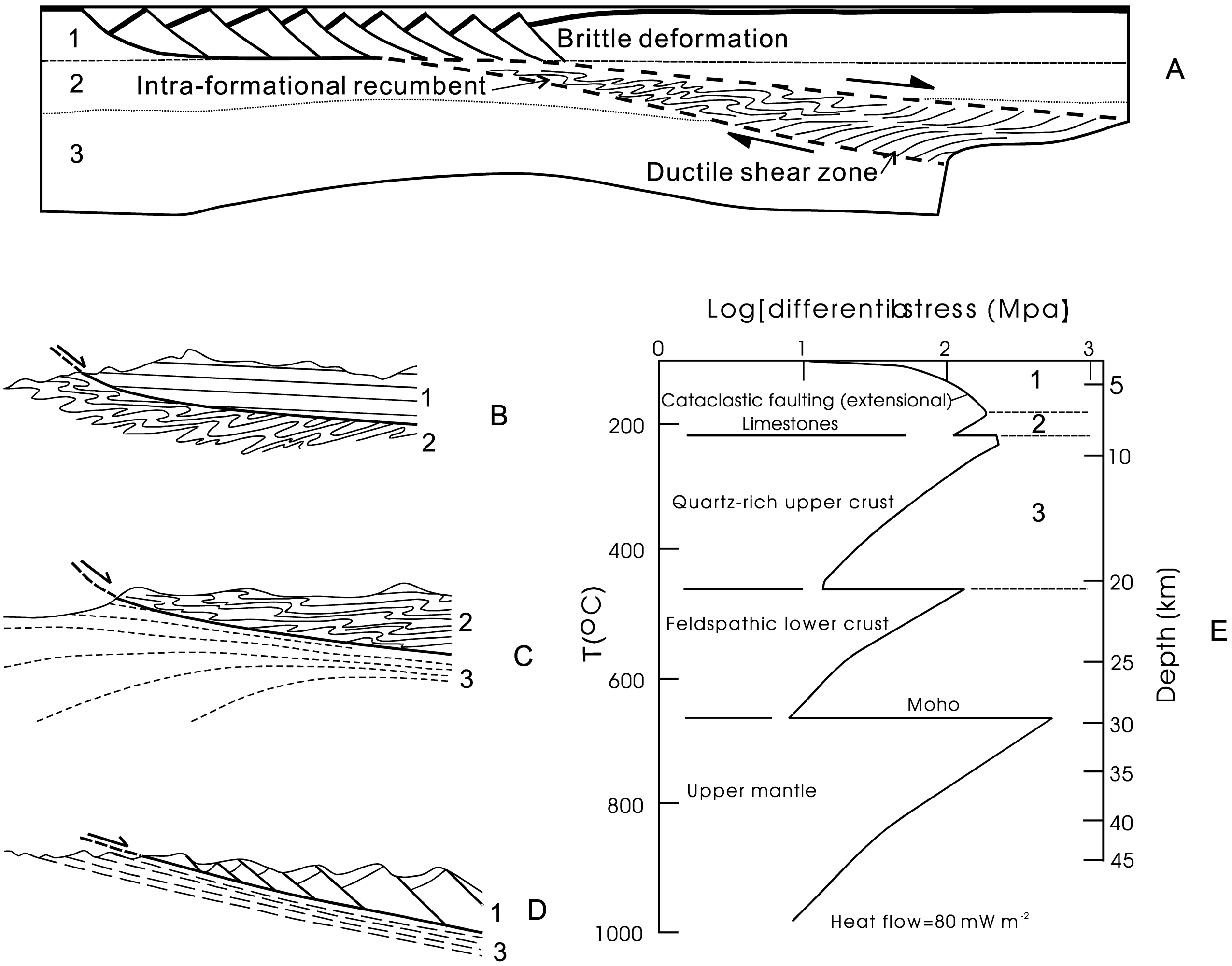

Fig. 11. An idealized configuration of crustal structure and development of extensional domes. (A) Early stage of extension of crustal layers 1, 2 and 3. (B) Least extension—the detachment faults thinned or removed some of the brittle sedimentary cover. (C) Modest extension—some of the middle ductily deformed slab has been thinned or removed. (D) Greatest extension: the middle ductily deformed slab has been removed, exemplified by the MCCs in the North America Cordillera. (E) Illustration of the deformation behavior and differentiation among the three layers of the JTD (after Rutter, 1993).

Formation (Fig. 2). The Xuanwei Formation is in turn conformably overlain by the Lower Triassic sequence. The omission of the Xuanwei Formation and lower Triassic sequence in the JDT can be explained by removal along the upper detachment fault, strongly supporting its interpretation as an extensional feature (Fig. 2).

In the North American Cordillera, metamorphic core complexes have a tectono-stratigraphic column with a brittly deformed upper plate, a mylonitically deformed lower plate, and a detachment fault between the two (Davis et al., 1980, 1986; Davis and Lister, 1988; Lister and Davis, 1989). They do not have middle ductily deformed slabs and thus, the three layer configuration in Jianglang (Fig. 11) is different from typical metamorphic core complexes. This difference can be explained by greater extension in the formation of typical metamorphic core complex than that observed in the JTD (Figs. 2 and 11D).

The JTD has a flat top and steep flanks suggesting that it is a superimposed fold (Fig. 4). The JTD occurs in a unique orogenic belt, which may have involved E–W compression, followed by southward thrusting during Cretaceous to Cenozoic time. The JTD differs from typical metamorphic core complexes in the North American Cordillera, where major post-orogenic extension took place in the Tertiary, and where doming of the MCCs accompanied regional extension (Davis and Lister, 1988; Lister and Davis, 1989).

4.2. Deformation sequences and their tectonic implications

The structural characteristics of the JTD are interpreted as reflecting at least five stages of deformation (Table 1). The earliest deformation in the schist complex (D_1), may have been extensional. It was followed by D_2, a compressional stage. A major extensional deformation (D_3) is recorded by the phyllonitic or mylonitic foliation (S_3) in the lower detachment zone and upper part of the schist complex, by the schistosity S'_1 in the middle slab, and by the brittle deformation in the upper detachment zone. All of the structures produced by D_1 through D_3 were reworked by later compressional deformation, which produced S_4 in the

Table 1
Deformation sequence of the Jianglang dome

Generation	Mesoproterozoic schist complex	Lower detachment	Sinian and Paleozoic Ductile middle slab	The Xikang Group
D_5 (?-today)	Brittle–ductile detachment, deformation of biotite porphyroblasts and the final exhumation of the JTD			
D_4 (115–131 Ma)	Buckling folding forming an elongate dome with its axis trending parallel to the orogenic belt, followed by southward thrusting			
D_3 (152–177 Ma)	Mylonitic foliation S_3 in detachment zone	Phyllonite foliation S_3	Bedding parallel foliation S'_1 Intra-layer recumbent folds and schistosity S'_1	Bedding S_0 Space and slaty cleavages S''_1
D_2 (184–192 Ma)	Asymmetric folds of S_1 and shallow dipping ductile shear zone, formation of S_2			
D_1(?) (>200 Ma)	Folding of S_0 and S_1 transposing S_0			

schist complex and in the middle slab and S''_1 in the Xikang Group. The final deformation (D_5) was extensional brittle–ductile deformation associated with thermometamorphism.

Identification of the Jianglang extensional dome has important implications for the tectonic reconstruction of the eastern margin of the Tibetan Plateau. The schist complex is a fragment of the lower plate that belongs to the Yangtze Block (Zhou et al., 2002). The earliest extension (D_1) might reflect rifting related to the Permian mantle plume that produced the voluminous Emeishan flood basalts (Chung and Jahn, 1995; Song et al., 2001). Following this extensional event, the Yangtze Block collided with the North China Block in the Triassic (Li et al., 1993), and part of its western margin was subducted beneath the Tibetan Plateau. The D_2 deformation may have been produced by this tectonic event at ca. 200 Ma as suggested by a structural study in Longmenshan (Dirks et al., 1994).

The upper and lower detachment faults mark the second stage of extension and reflect an important tectonic event in this area. This extension may have caused the thinning and variable omission of strata in the JTD and its exhumation. This major extension event was recently dated at 177 ± 3 Ma using the SHRIMP zircon dating method (Zhou et al., 2002). Such an age is consistent with previous K–Ar dates on illite from the Xikang Group ranging from 152 to 177 Ma (SBGMR, 1991). The illite is associated with the D_3 deformation represented by S_3 in the lower detachment zone and schist complex, S'_1 in the middle slab, and brittle deformation in the upper detachment zone (Table 1). The detachment faults are also locally intruded by granites (Fig. 3), which have been dated at 115, 118 and 131 Ma (SBGMR, 1991).

The ESE-oriented mineral lineations and sheath folds, which indicate the maximum stretching direction (Jiang and Williams, 1999) in the upper part of the schist complex, the lower detachment zone and the middle slab (Fig. 3), are similar to scratches in the upper detachment zone. These features suggest that the ESE extension and detachment faulting may have occurred during the middle-Jurassic, coincident with uplift of the JTD at 177 Ma.

The final stage of extension (D_5) is believed to have resulted from the collision between Eurasia and India. Such a collision may have produced the sinistral strike-slip faulting and extrusion tectonics in the region (Tapponnier et al., 1982). This stage of deformation was associated with the uplift of the Tibetan Plateau (Mattauer et al., 1992).

5. Conclusions

1. The JTD has three tectono-stratigraphic units, an inner schist complex, a middle ductily deformed slab and a sedimentary cover unit. These three units are separated from one another by extensional detachment faults.
2. Five generations of deformation are recorded by a sequence of foliations. The earliest extension, (D_1) in the

schist complex, probably occurred prior to collision of the South and North China Blocks. The compressional phase D_2 was related to subduction of the Yangtze Block beneath the eastern margin of the Tibetan Plateau during the Indosinian Orogeny. A major extensional deformation (D_3) was associated with regional detachment faulting and may have caused thinning and selective removal of the Sinian and Paleozoic strata and exhumation of the tectonic dome at 177–152 Ma. The compressional event D_4 was followed by the extension deformation of D_5, which was associated with the India–Eurasia collision.

3. The JTD occurs in a unique orogenic belt, which underwent E–W compression, followed by southward thrusting during Cretaceous to Cenozoic. Emplacement of the JTD may have been related to both extensional and compressional deformation. The JTD differs from typical MCCs in the North American Cordillera, where a major post-orogenic extension took place in the Tertiary, and where doming of the MCCs accompanied regional extension.

Acknowledgments

This study was supported by research grants from the KLLTE of China University of Geosciences, the NSF of China (project 40172070 to DPY and a young researcher award to MFZ), and the Research Grant Council of Hong Kong SAR (HKU7101/01P and HKU7124/02P to MFZ). We benefited from discussions with Prof. Luo Yaonan of the Geological Survey of Sichuan Province and Prof. Wu Zhenwen of the China University of Geosciences (Beijing). We are grateful to J. Ali, G.A. Davis, M.A. Edwards, G.S. Lister, B. Rhodes, and P.T. Robinson for critical but constructive comments that improved the manuscript.

References

Allen, C.R., Luo, Z.L., Qian, H., Wen, Y., Zhou, H., Huang, W., 1991. Field study of a highly active fault zone: the Xian Shui He fault of southwestern China. Geological Society of American Bulletin 103, 1178–1199.

Avigad, D., 1995. Exhumation of the Dabie Shan ultra-high-pressure rocks and accumulation of the Songpan Garze flysch sequence, Central China: comment. Geology 23, 764–765.

Bruguier, O., Lancelot, J.R., Malavieille, J., 1997. U–Pb dating on single detrital zircon grains from the Triassic Songpan–Garze flysch (Central China): provenance and tectonic correlations. Earth and Planetary Science Letters 152, 217–231.

Burchfiel, B.C., Chen, Z., Liu, Y., Royden, L.H., 1995. Tectonics of the Longmenshan and adjacent regions, Central China. International Geology Review 37, 661–736.

Chang, E.Z., 2000. Geology and tectonics of the Songpan–Ganzi fold belt, Southwestern China. International Geology Review 42, 813–831.

Chen, S.F., Wilson, C.J.L., 1996. Emplacement of the Longmenshan Thrust–Nappe belt along the eastern margin of the Tibetan Plateau. Journal of Structural Geology 18, 413–430.

Chen, S.F., Wilson, C.J.L., Worley, B.A., 1995. Tectonic transition from the Songpan–Garze fold belt to the Sichuan basin, south-western China. Basin Research 7, 235–253.

Chung, S.L., Jahn, B.M., 1995. Plume–lithosphere interaction in generation of the Emeishan flood basalts at the Permian–Triassic boundary. Geology 23, 889–892.

Davis, G.A., Lister, G.S., 1988. Detachment faulting in continental extension: Perspectives from the southwestern U.S. Cordillera. In: Clark, S.P., Burchfiel, B.C., Suppe, J. (Eds.), Processes in Continental Lithospheric Deformation. Special Paper—Geological Society of America, 218, Boulder, CO, pp. 133–159.

Davis, G.A., Anderson, J.L., Frost, E.G., Shackleford, T.J., 1980. Mylonitization and detachment faulting in the Whipple Buckskin Rawhide Mountains terrane, Southeastern California and Western Arizona. Geological Society of America Memoir 153, 79–129.

Davis, G.A., Lister, G.S., Reynolds, S.J., 1986. Structural evolution of the Whipple and South mountains shear zones, southwest United States. Geology 14, 7–10.

Dirks, P.H.G.M., Wilson, C.J.L., Chen, S., Luo, Z.L., Liu, S., 1994. Tectonic evolution of the NE margin of the Tibetan Plateau, evidence from the central Longmen mountains, Sichuan province, China. Journal of Southeast Asian Earth Sciences 9, 181–192.

Fu, Z.R., Song, H.L., Yan, D.P., 1997. The structure of the Jianglang metamorphic core complex in the western margin of the Yangtze platform and its control on mineralization. Acta Geologica Sinica 71, 113–122.(in Chinese).

Hou, L.W., 1996. Type and Genesis of domal deformational–metamorphic terranes in the western margin of the Yangtze craton. In: Luo, Y.N., (Ed.), Contributions to Geology and Mineral Resources in an Intracontinental Orogenic Belt on the SW Margin of the Yangtze Block, Sichuan Science and Technology Press, Chengdu, China, pp. 13–27, (in Chinese).

Huang, M.H., Hou, L.W., Fu, X.F., 1996. P–T–t–D Path of metamorphic terranes in the Danba area. In: Luo, Y.N., (Ed.), Contributions to Geology Mineral Resources in an Intracontinental Orogenic Belt on the SW Margin of the Yangtze Block, Sichuan Science and Technology Press, Chengdu, China, pp. 41–50, (in Chinese).

Jiang, D.Z., Williams, P.F., 1999. When do dragfolds not develop into sheath folds in shear zones? Journal of Structural Geology 21, 577–583.

Lacassin, R., Scharer, U., Leloup, P.H., Arnaud, N., Tapponnier, P., Liu, X.H., Zhang, L.S., 1996. Tertiary deformation and metamorphism, SE of Tibet: the folded tiger-leap decollement of NW Yunnan, China. Tectonics 15, 605.

Li, S., Chen, Y., Cong, B., Zhang, Z., Zhang, R., Liou, D., Hart, S.R., Ge, N., 1993. Collision of the North China and the Yangtze Blocks and formation of coesite-bearing eclogites: timing and processes. Chemical Geology 109, 70–89.

Lister, G.S., Davis, G.A., 1989. The origin of metamorphic core complexes and detachment faults formed during tertiary continental extension in the northern Colorado River region, USA. Journal of Structural Geology 11, 65–94.

Lister, G.S., Etheridge, M.A., Symonds, P.A., 1991. Detachment models for the formation of passive continental margins. Tectonics 10, 1038–1064.

Liu, H.F., Lian, H.S., Cai, L.G., Shen, F., 1994. Structural styles of the Longmenshan thrust belt and evolution of the foreland basin in the western Sichuan Province, China. Acta Geologica Sinica 68, 101–118. (in Chinese).

Mattauer, M., Malavieille, J., Calassou, S., Lancelot, J., Roger, F., Hao, Z.W., Xu, Z.Q., Hou, L.W., 1992. The Songpan–Garze Triassic belt of west Sichuan and eastern Tibet—a decollement fold belt on passive margin. Comptes Rendus Delacademe des Sciences II 314, 619–626.

Nie, S., Yin, A., Rowley, D.B., Jin, Y., 1994. Exhumation of the Dabie Shan ultra-high-pressure rocks and accumulation of the Songpan Garze flysch sequence, central China. Geology 22, 999–1002.

Nie, S., Yin, A., Rowley, D.B., Jin, Y., 1995. Exhumation of the Dabie Shan ultra-high-pressure rocks and accumulation of the Songpan Garze flysch sequence, central China: reply. Geology 23, 765–766.

Ramsay, J.G., Huber, M.I., 1987. The Techniques of Modern Structural Geology—Volume 2: Fold and Fracture, Academic Press, pp. 347–363.

Roger, F., Calassous, S., Lancelot, J., Malavieille, J., Mattauer, M., Xu, Z.Q., Hao, Z.W., Hou, L.W., 1995. Miocene emplacement and deformation of the Kongashan granite (Xianshuihe fault zone, west Sichuan, China)—geodynamic implications. Earth and Planetary Science Letters 130, 201–216.

Rutter, E.H., 1993. The mechanics of natural rock deformation. In: Hudson, J.A., (Ed.), Comprehensive Rock Engineering: Principle, Practice, and Projects, Oxford, Pergamon Press, pp. 63–109.

SBGMR (Sichuan Bureau of Geology and Mineral Resources), 1991. Regional Geology of Sichuan Province, Geological Publishing House, Beijing, China, pp. 1–680, (in Chinese).

Song, H.L., Yan, D.P., Fu, Z.R., 1996. Metamorphic core complexes in the western margin of the Yangtze craton. In: Progress in Geology of China (1993–1996)—Papers to 30th International Geological Congress, China Ocean Press, Beijing, China, pp. 370–373.

Song, X.Y., Zhou, M.-F., Hou, Z.Q., Cao, Z.M., Wang, Y.L., Li, Y.Q., 2001. Geochemical constraints on the mantle source of the upper Permian Emeishan continental flood basalts, SW China. International Geology Review 43, 213–225.

Spencer, J.E., 1984. Role of tectonic denudation in Warping and uplifting of low-angle normal fault. Geology 12, 95–98.

Tapponnier, P., Peltzer, G., Le Dain, A.Y., Armijo, R., Cobbold, P., 1982. Propagating extrusion tectonics in Asia: new insights from simple experiments with plasticine. Geology 10, 611–616.

Wang, E., Burchfiel, B.C., 2000. Late Cenozoic to Holocene deformation in southwestern Sichuan and adjacent Yunnan, China, and its role in formation of the southeastern part of the Tibetan Plateau. Geological Society of America Bulletin 112, 413–423.

Wang, E., Burchfiel, B.C., Royden, L.H., Chen, L., Chen, J., Li, W., Chen, Z., 1998. Late Cenozoic Xianshuihe–Xiaojiang, Red River, and Dali Fault Systems of Southwestern Sichuan and Central Yunnan, China, Geological Society of America, pp. 6–39.

Wang, X., Metcalfe, I., Jian, P., He, L., Wang, C., 2000. The Jinshajiang–Ailaoshan suture zone, China: tectonostratigraphy, age and evolution. Journal of Asian Earth Sciences 18, 675–690.

Wernicke, B., 1990. The fluid crustal layer and its implications for continental dynamics. In: Salisbury, M.H., Fountain, D.M. (Eds.), Exposed Cross-sections of the Continental Crust, Kluwer Academic Publisher, The Netherlands, pp. 509–544.

Wernicke, B., Axen, G.J., 1988. On the role of isostasy in the evolution of normal fault systems. Geology 16, 848–851.

Wernicke, B., Axen, G.J., Snow, J.K., 1988. Basin and Range extension tectonics at the latitude of Las Vegas, Nevada, In: Geological Society of America, 1888–1988, Centennial Article, pp. 243–262.

Worley, B.A., Wilson, C.J.L., 1996. Deformation partitioning and foliation reactivation during transpressional orogenesis, an example from the central Longmen Shan, China. Journal of Structural Geology 18, 395–411.

Xu, Z.Q., Hou, L.W., Wang, Z.X., 1992. Orogenic Processes of the Songpan–Garze Orogenic Belt of China, Geological Publisher House, Beijing, China, pp. 7–137, (in Chinese).

Yan, D.-P., Song, H.L., Fu, Z.R., Tian, J.Y., Du, Y.J., Luo, L., 1996. Reinterpretation of "Stratigraphy" in the Jianglang dome, Jiulong, Sichuan Province. In: Luo, Y.N., (Ed.), Contributions to Geology and Mineral Resources in Intracontinental Orogenic Belt on the SW Margin of the Yangtze Block, Sichuan Science and Technology Press, Chengdu, China, pp. 58–66, (in Chinese).

Yan, D.-P., Song, H.L., Fu, Z.R., Tian, J.Y., 1997. Metamorphic Core Complexes in the Western Margin of the Yangtze Craton, Geological Publisher House, Beijing, China, pp. 6–72, (in Chinese).

Yin, A., 1989. Origin of regional rooted low-angle normal faults: a mechanical model and its tectonics implications. Tectonics 8, 469–482.

Zhang, Y., Luo, Y.N., Yang, C.X., 1990. Panxi Rift and its Geodynamics, Geological Publisher House, Beijing. China, p. 415.

Zhou, M.-F., Yan, D.-P., Kennedy, A.K., Li, Y.Q., Ding, J., 2002. SHRIMP U–Pb zircon geochronological and geochemical evidence for Neoproterozoic arc-magmatism along the western margin of the Yangtze block, South China. Earth and Planetary Science Letters 196, 51–67.